AIP | Journal of Applied Physics

Effect of sputtered lanthanum hexaboride film thickness on field emission from metallic knife edge cathodes

M. P. Kirley, B. Novakovic, N. Sule, M. J. Weber, I. Knezevic et al.

Citation: J. Appl. Phys. **111**, 063717 (2012); doi: 10.1063/1.3698281
View online: http://dx.doi.org/10.1063/1.3698281
View Table of Contents: http://jap.aip.org/resource/1/JAPIAU/v111/i6
Published by the American Institute of Physics.

Related Articles

Breakdown voltage reliability improvement in gas-discharge tube surge protectors employing graphite field emitters
J. Appl. Phys. 111, 083301 (2012)

Space charge and quantum effects on electron emission
J. Appl. Phys. 111, 054917 (2012)

Enhanced electron field emission from plasma-nitrogenated carbon nanotips
J. Appl. Phys. 111, 044317 (2012)

Field-emission properties of individual GaN nanowires grown by chemical vapor deposition
J. Appl. Phys. 111, 044308 (2012)

High emission currents and low threshold fields in multi-wall carbon nanotube-polymer composites in the vertical configuration
J. Appl. Phys. 111, 044307 (2012)

Additional information on J. Appl. Phys.

Journal Homepage: http://jap.aip.org/
Journal Information: http://jap.aip.org/about/about_the_journal
Top downloads: http://jap.aip.org/features/most_downloaded
Information for Authors: http://jap.aip.org/authors

ADVERTISEMENT

Downloaded 19 Apr 2012 to 128.104.180.67. Redistribution subject to AIP license or copyright; see http://jap.aip.org/about/rights_and_permissions

Effect of sputtered lanthanum hexaboride film thickness on field emission from metallic knife edge cathodes

M. P. Kirley,[a] B. Novakovic, N. Sule, M. J. Weber, I. Knezevic, J. H. Booske
Department of Electrical and Computer Engineering, University of Wisconsin-Madison, Madison, Wisconsin 53706, USA

(Received 11 November 2011; accepted 23 February 2012; published online 28 March 2012)

We report experiments and analysis of field emission from metallic knife-edge cathodes, which are sputter-coated with thin films of lanthanum hexaboride (LaB_6), a low-work function material. The emission current is found to depend sensitively on the thickness of the LaB_6 layer. We find that films thinner than 10 nm greatly enhance the emitted current. However, cathodes coated with a thicker layer of LaB_6 are observed to emit less current than the uncoated metallic cathode. This result is unexpected due to the higher work function of the bare metal cathode. We show, based on numerical calculation of the electrostatic potential throughout the structure, that the external (LaB_6/vacuum) barrier is reduced with respect to uncoated samples for both thin and thick coatings. However, this behavior is not exhibited at the internal (metal/LaB_6) barrier. In thinly coated samples, electrons tunnel efficiently through both the internal and external barrier, resulting in current enhancement with respect to the uncoated case. In contrast, the thick internal barrier in thickly coated samples suppresses current below the value for uncoated samples in spite of the lowered external barrier. We argue that this coating thickness variation stems from a relatively low (no higher than 10^{18} cm^{-3}) free carrier density in the sputtered polycrystalline LaB_6. © *2012 American Institute of Physics*. [http://dx.doi.org/10.1063/1.3698281]

I. INTRODUCTION

Electron emission from a surface requires that an electron overcome the energy barrier between vacuum and the conduction band of the emitting material. This process can occur in a variety of ways, including thermal emission and field emission.[1] Field emission takes place when an electron tunnels through the energy barrier that has been narrowed by an intense electric field. Electron emission depends very strongly on the work function of the emitter material, essentially the height of the energy barrier. Cathodes made from a low-work function material exploit this dependence to produce greater emission.[1] The Fowler-Nordheim equation is a one-dimensional approximation relating the field emission current density J to the applied electric field F, and states that the current is proportional to the inverse exponential of the work function ϕ,[2,3]

$$J(F) = \frac{q\sqrt{\mu/\phi}}{4\pi^2\hbar(\mu+\phi)}F^2 \exp\left(-\frac{4}{3\hbar F}\sqrt{2m\phi^3}\right), \qquad (1)$$

where q is the electron charge, m is the electron mass, and μ is the chemical potential.

Lanthanum hexaboride (LaB_6) has been widely used as a thermionic and field emitter due to its low work function ($\phi \approx 2.66$ eV) and high melting temperature.[4] Bulk LaB_6 emitters can be fabricated from single crystals[5] or by sintering powdered LaB_6,[6] and are used in applications like electron microscopes[7] and free electron lasers.[8] LaB_6 coatings are created using a variety of methods, such as pulsed laser deposition,[9] molecular beam epitaxy,[7] and sputtering.[10] The microstructure and thermionic emission properties of sputtered LaB_6 films have been well studied, and LaB_6 coatings used as thermionic emitters have been shown to enhance field emission with respect to uncoated cathodes.[11–13] The electrical properties of LaB_6 thin films have been characterized, but these results depend sensitively on the deposition method and parameters. Kato *et al.* found resistivity values ranging from 2.2×10^{-4} to 6.0×10^{-4} Ω-cm for LaB_6 films deposited using laser molecular beam epitaxy.[7] Peschmann *et al.* measured a resistivity of 1.33×10^{-4} Ω-cm for bulk LaB_6 and resistivities between 0.52×10^{-4} and 2.00×10^{-4} for films between 13 and 204 nm produced by sputtering or electron beam evaporation.[14] Winsztal *et al.* measured a resistivity of 0.07×10^{-4} Ω-cm for single crystal bulk LaB_6. They measured sputtered amorphous and polycrystalline films that had resistivities ranging from 0.35×10^{-4} Ω-cm to 10×10^{-4} Ω-cm. They also produced very thin sputtered LaB_6 films (less than 50 nm) with extremely high resistivities up to 10^6 Ω-cm.[15] Carbon nanotubes sputter-coated with LaB_6 have been shown to increase field emission compared to the uncoated case.[16] However, a study of whether the emission depends on the coating thickness has not been performed previously. Possible applications of LaB_6 field emitters include flat-panel displays,[16] improved performance electron microscopes,[17] and micron-sized electron emitters for vacuum electronics.[9]

In this work, we show that the field emission from LaB_6-coated metallic knife edge cathodes is enhanced with respect to uncoated cathodes. However, the emission depends sensitively on the thickness of the sputter-coated layer, and enhancement only occurs for films thinner than

[a]Author to whom correspondence should be addressed. Electronic mail: kirley@wisc.edu.

 © 2012 American Institute of Physics

Downloaded 19 Apr 2012 to 128.104.180.67. Redistribution subject to AIP license or copyright; see http://jap.aip.org/about/rights_and_permissions

10 nm. This finding contradicts the expectation that the low work function of the LaB_6, with respect to the metal, will cause increased emission regardless of the coating thickness. We explain this result based on calculations of the electrostatic potential throughout the structure. These simulations show that the external (LaB_6/vacuum) barrier is reduced with respect to uncoated samples for both thin and thick coatings, allowing efficient electron tunneling into vacuum. In contrast, the efficiency of electron tunneling through the internal (metal/LaB_6) barrier depends on the coating thickness, becoming extremely poor for very thick coatings. As a result, in thinly coated samples, electrons tunnel efficiently through both the internal and external barrier, producing current enhancement with respect to the uncoated case. The thick internal barrier in thickly coated samples, however, suppresses current below the value for uncoated samples despite the lowered external barrier. We argue that this emission current variation stems from a relatively low (no higher than 10^{18} cm^{-3}) free carrier density in the sputtered polycrystalline LaB_6.

This paper is organized in the following manner: In Sec. II, we describe the methods of cathode fabrication and field emission current measurement. Section III contains the results and discussion of field emission current and x-ray diffraction (XRD) measurements of the cathodes. In Sec. IV, we describe our method of calculating the electrostatic potential in the metal-LaB_6-vacuum system. Section V contains simulation results and our explanation of the observed phenomena. Our conclusions are summarized in Sec. VI.

II. EXPERIMENTAL METHODS

The knife-edge cathodes under study were fabricated using electro-discharge machining of copper (Cu). An optical image of a cathode is shown in Fig. 1. The knife edges are 0.13 mm thick and 0.75 mm high, with a spacing of 0.77 mm. The cathodes were cleaned in an ultrasonic acetone bath and rinsed with isopropyl alcohol before being coated with LaB_6. Direct current magnetron sputtering was used to deposit 75 nm of titanium (Ti) as an adhesion layer, followed by a thin LaB_6 film. The LaB_6 film was deposited while the substrate was heated to 200 °C.[13] The deposition rate of LaB_6 was calibrated by performing deposition on a polished silicon wafer which was partially masked. After removing the mask, the resulting layer thickness was measured using a profilometer with 0.5 nm resolution. At 3 mTorr argon pressure and sputtering power of 700 W, the deposition rate was 11 nm/min.

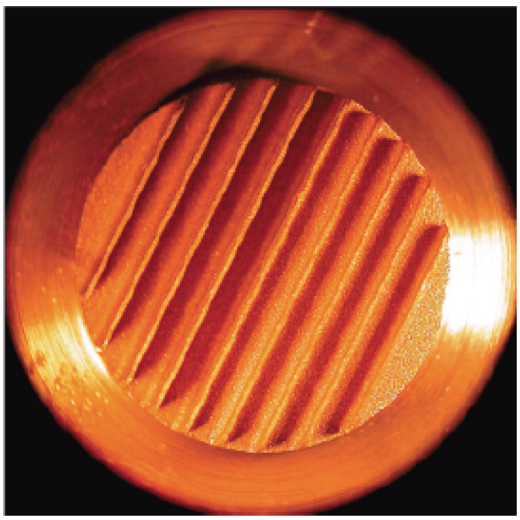

FIG. 1. Photograph of uncoated knife edge cathode.

The experiments were performed in an ultrahigh vacuum (UHV) chamber with base pressures on the order of 10^{-10} Torr. The cathode was mounted in the UHV system on an x-y-z translation stage. Anode-cathode spacing was zeroed by placing the sample in contact with the anode, as determined by electrical resistance measurement. The anode-cathode spacing for all measurements was 0.250 mm $\pm$ 0.013 mm. The cathode base diameter is 1.6 cm. The anode is a flat metal plate with a diameter of 2.5 cm. In order to make a direct comparison between cathodes, the emission area must be the same for each sample. Microscale roughness and misalignment can cause the emission area to vary between samples, because these features would introduce variation in the anode-cathode spacing between samples. A phosphor screen would allow observation of emission uniformity from sample to sample, but we were unable to implement such a system due to equipment and cost constraints. Despite these concerns, we are confident that the data can be interpreted unambiguously. Emission from isolated protrusions would likely cause local heating and ablation of the surface, resulting in surface morphology change and significant fluctuations in total emission current, which we did not observe. We followed a consistent procedure to minimize misalignment errors. The anode is fixed and the cathode is mounted on a 3 axis positioning stage. We mounted the cathodes such that the knife edges were oriented in the same direction, and used the same fabrication process for all the cathodes. Pulsed high voltage was supplied by a 10 kV power supply and fast high voltage switch. Measurements were performed with a pulse width of 8 ms at a rate of 22.0 Hz. We chose to perform pulsed measurements because we were concerned about the uncertainty that could be introduced due to heating of the cathode under DC operation. We sought to minimize material composition changes due to heating and surface morphology changes due to thermal cycling. A custom three-stage amplifier circuit was used to detect total field emission currents as low as several nanoamps. Field emission measurements were performed from the first detectable emission up to 10 kV external applied voltage.

III. EXPERIMENTAL RESULTS

Figure 2 presents a plot of emission current versus applied voltage. One can observe that emission current is enhanced for the cathodes coated with less than 10 nm of LaB_6, and the enhancement increases with decreasing coating thickness. With respect to a knife-edge cathode that had been coated only with Ti ($\phi = 4.3$ eV),[18] the thinnest film exhibited emission current 20 times greater. According to the Fowler-Nordheim theory, the cathode material with a

Downloaded 19 Apr 2012 to 128.104.180.67. Redistribution subject to AIP license or copyright; see http://jap.aip.org/about/rights_and_permissions

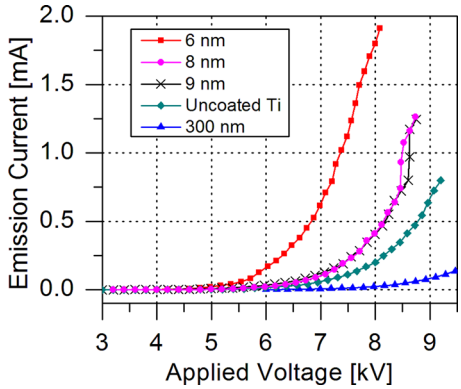

FIG. 2. I-V characteristics of cathodes with different thicknesses of the LaB_6 coating. Emission is greatly enhanced for thin films and suppressed for thick films.

lower work function should always exhibit higher emission, but we observed that thick coating layers suppressed field emission. Specifically, cathodes with ~300 nm thick LaB_6 coatings produce far less current than the bare metal (Ti-coated Cu) cathode.

We expect our film to have fine-grained polycrystalline to amorphous structure and stoichiometry closer to LaB_7 than LaB_6.[10,12] Figure 3 presents the XRD data for the cathode with a 300 nm thick LaB_6 coating. One can observe the peaks due to the Cu cathode, the Ti adhesion layer, and the LaB_6 coating. X-rays will penetrate the surface to a depth of between one and several hundred micrometers[19] depending on the test material, thus the Cu peaks are much larger than the others. The presence of the LaB_6 diffraction peaks indicates that the coating possesses polycrystalline structure. The relatively small amplitude of these peaks is likely due to the thinness of the coating, but the low peak amplitude could also result from a highly disordered, extremely fine-grained, non-stoichiometric structure.

IV. SIMULATION METHODS

We hypothesized that the unexpected emission behavior for different coating layer thicknesses occurred due to an electron transport barrier at the internal (Ti/LaB_6) interface. In order to test this hypothesis, we calculated the spatial variation of the conduction band minimum in the Ti, in the LaB_6 coating, and in vacuum. We performed this calculation for

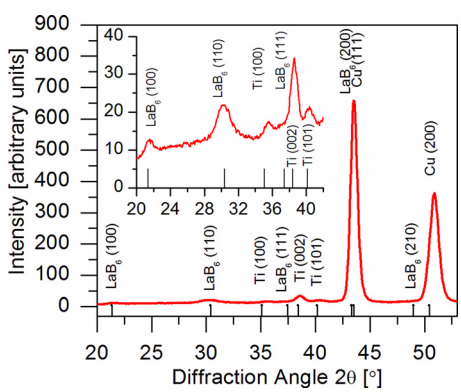

FIG. 3. XRD pattern of a LaB_6 coated cathode.

several film thicknesses with charge carrier density in the LaB_6 film as a variable parameter. A direct determination of the mobile charge carrier density in the LaB_6 films was not possible with available measurement facilities, because the very thin films and metallic substrate precluded definitive measurements of electronic properties. As a starting point, we assumed the mobile electron density of ideal crystalline LaB_6 ($n = 1.5 \times 10^{22}$ cm^{-3}).[20] However, other experimental works have observed increased resistivity in LaB_6 thin films[7,14,15] with respect to bulk material.[21,22] As will be discussed, our experimental data and computational modeling support the hypothesis of a significantly lower conduction electron density in the as-deposited film due to defects, disorder, and non-stoichiometry.

Our numerical electron transport model calculates the potential inside the cathode materials by using the Thomas-Fermi approximation of Poisson's equation.[23–25] The potential in vacuum is calculated by using the method of images.[26] In the Ti and LaB_6, we calculate the density of states by using periodic boundary conditions.[27] We take the density-of-states effective mass in LaB_6 to be half the free electron mass, $m^*_{LaB6} = 0.5 \times m_0$.[28,29] The electron affinity in LaB_6 is assumed to be 3.5 eV. Titanium is a transition metal (partially filled atomic *d*-shell) and has a complicated band structure.[30–35] Furthermore, the Fermi level falls in the energy region of *d*-derived energy bands.[30–35] These bands are highly non-parabolic and have a much higher density of states with respect to a free electron band (they are much narrower in energy).[30–35] Four valence electrons per atom are delocalized and fill the Ti crystal energy bands, while the Fermi energy is about 6.5 eV.[33–35] Since the Ti mass density is $\rho = 4.5$ g/cm^{-3} and its atomic weight is 47.867 in atomic mass units,[18] $A = 47.867$ g/mol. We can use the following equation to calculate the mobile electron density:

$$n = 4\frac{\rho}{A}N_A = 2.26 \cdot 10^{23}\ \text{cm}^{-3}, \tag{2}$$

where $N_A = 6.022 \times 10^{23}$ is the Avogadro number (number of atoms in one mole). To fit the Ti band structure, with $E_F = 6.5$ eV and $n = 2.26 \times 10^{23}$ cm^{-3}, in our free electron model where the underlying crystal lattice is accounted for through an effective mass, the appropriate effective mass for Ti must be $m^* = 2.08 \times m_0$. In order to solve the Poisson equation throughout the Ti/LaB_6/vacuum structure, the dielectric constant (the real part of the dielectric function) must be specified in each layer. The static dielectric constant of good metals is well approximated by unity, and we adopt this value both for the metallic Ti and for the semi-metallic LaB_6.

V. SIMULATION RESULTS

We compare our observations of enhanced (suppressed) emission for films thinner (thicker) than 10 nm with predictions from the theoretical model. In all electron potential plots, 0 eV is defined as the bottom of the conduction band in the Ti; the left region is the Ti, the middle region is the LaB_6 layer, and the rightmost region is vacuum. At room temperature, only electrons with energy near the Fermi level

Downloaded 19 Apr 2012 to 128.104.180.67. Redistribution subject to AIP license or copyright; see http://jap.aip.org/about/rights_and_permissions

are involved in conduction and the interface between the metal and the coating presents a barrier to transport. When the LaB_6 and the Ti are brought into contact, free conduction electrons in the LaB_6 conduction band diffuse into lower energy states in the metal. This diffusion causes conduction band minimum bending in the coating and sets up a built-in voltage difference at the internal interface. Some electrons remain in the LaB_6 film after diffusion. The external electric field is screened at the external (LaB_6/vacuum) interface by these electrons.

In the simulations of coating films with a high ($n = 6 \times 10^{18}$ cm^{-3}) carrier density, electron diffusion proceeds upon contact until the Fermi levels in the coating and the substrate equilibrate. Many electrons are available to diffuse, resulting in a large built-in voltage and a tall, narrow potential barrier at the interface. This effect occurs in single-crystalline LaB_6 emitters; the carrier density of the crystal is high enough such that an Ohmic contact, rather than a Schottky contact, is formed when the LaB_6 is put in contact with a metal. Electrons can tunnel easily back and forth between the metal and the LaB_6 coating, ensuring a supply of electrons at the external interface to be field emitted. Upon the application of an electric field, the potential barrier at the external interface is lowered and narrowed, and electrons in the coating tunnel into vacuum. Due to the high carrier density, the applied electric field is screened at the external interface. This screening will occur both for thick films and very thin films. As a result of this screening, the shape of the potential at the internal interface will not be affected by the applied electric field. Simulations of coatings with high mobile electron densities resulted in electron potentials with these features, as shown in Fig. 4. The calculated potentials show that the barrier shape at the internal interface is independent of the coating layer thickness. Since LaB_6 has a lower work function than the metal, and because the internal barrier does not present a significant barrier to electron transport, the resulting emission would be enhanced with respect to the bare metal cathode for all coating layer thicknesses and would not vary as a function of coating layer thickness. Both of these results contradict experimental findings.

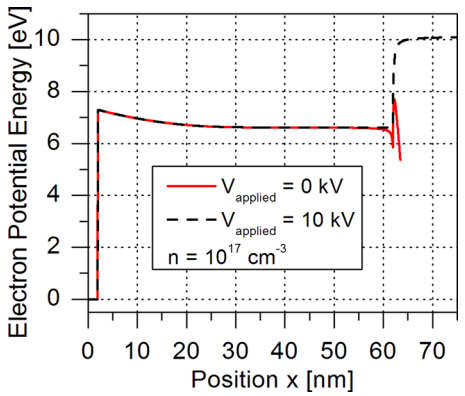

FIG. 5. Simulated electron potential energy as a function of position for a thick LaB_6 coating with a low carrier density ($n = 1 \times 10^{17}$ cm^{-3}). The potential near the internal interface (located at 2 nm) does not change shape when an electric field is applied.

In the simulations of thick coating films with a low ($n = 1 \times 10^{17}$ cm^{-3}) carrier density, electron diffusion proceeds upon contact until the Fermi levels in the coating and the substrate equilibrate. However, fewer electrons are available to diffuse, resulting in a large built-in voltage and a tall, thick potential barrier at the internal interface. Tunneling probability decays rapidly with increasing barrier width, so the thick potential barrier impedes electron tunneling through the internal interface. Upon the application of an electric field, the potential barrier at the external interface is lowered and narrowed, and electrons in the coating can tunnel into vacuum. Despite the low carrier density of the film, the large thickness of the film provides sufficient electrons at the surface to screen the electric field out of the coating, as shown in Fig. 5.

In the simulations of thin coating films with a low carrier density, electron diffusion proceeds upon contact until all free conduction electrons from the LaB_6 diffuse into the metal. Very few electrons are available to diffuse, however,

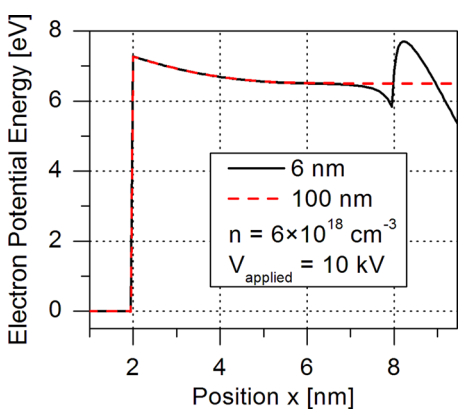

FIG. 4. Simulated electron potential energy as a function of position for a thin (black solid curve) and a thick (red dashed curve) LaB_6 coating, where the film is assumed to have a high carrier density ($n = 6 \times 10^{18}$ cm^{-3}). The applied electric field is screened out at the surface and the potential near the internal interface (located at 2 nm) is unaffected by the field.

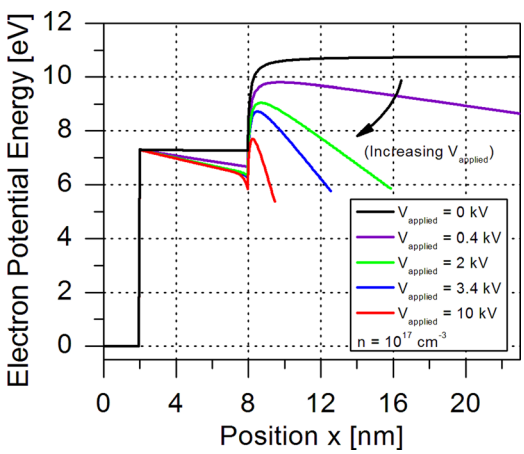

FIG. 6. Simulated electron potential energy as a function of position for a thin LaB_6 coating with a low carrier density ($n = 1 \times 10^{17}$ cm^{-3}). Band bending in the LaB_6 ceases when significant tunneling from the metal occurs.

Downloaded 19 Apr 2012 to 128.104.180.67. Redistribution subject to AIP license or copyright; see http://jap.aip.org/about/rights_and_permissions

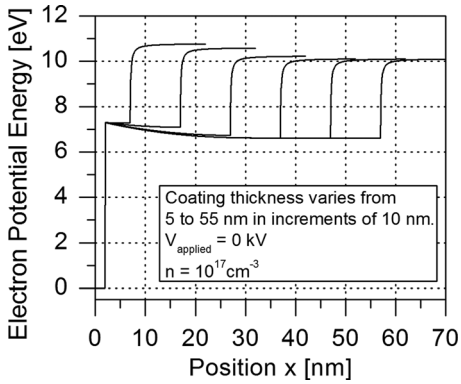

FIG. 7. Simulated electron potential energy as a function of position for several LaB_6 coating thicknesses at zero applied electric field and a low carrier density ($n = 1 \times 10^{17}$ cm^{-3}). Band bending due to diffusion is reduced when the coating layer is very thin.

resulting in a very small built-in voltage and a step-shaped potential barrier at the internal interface, as shown in Fig. 6. An applied electric field then penetrates into the thin film because the coating layer is depleted of free charge carriers. As the field strength is increased, the potential barrier at the external interface is lowered and narrowed, while simultaneously the conduction band energy minimum in the LaB_6 layer is bent downward. This band bending ceases when the internal barrier is thin enough such that a significant number of electrons tunnel into the LaB_6 film, gather at the external interface and screen any additional applied electric field. Figure 6 illustrates a simulation where this charge accumulation in the thin LaB_6 film screens the applied electric field when the external bias voltage is greater than 2 kV. Any further increase in the applied electric field affects only the external barrier shape.

The calculated potentials for low-free-carrier-density films show that the shape of the potential energy barrier at the internal interface is dependent on the coating layer thickness, as shown in Fig. 7. In the thick and thin film cases, band bending due to electron diffusion and field penetration pull the metal Fermi level closer to the vacuum level, effectively reducing the work function. This lowering of the work function is shown in Fig. 8 for a thin film. In this case,

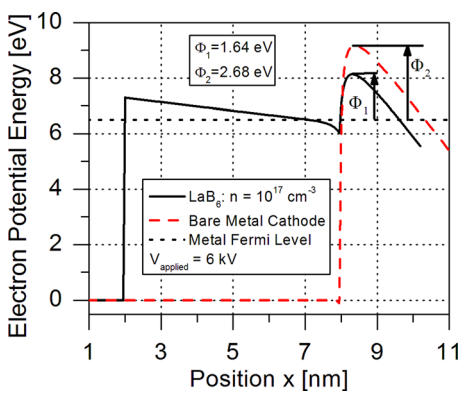

FIG. 8. Simulated electron potential energy as a function of position for a coated and an uncoated cathode. Conduction band minimum bending in the LaB_6 draws the Fermi level in the metal closer to the vacuum level, effectively reducing the work function of the system.

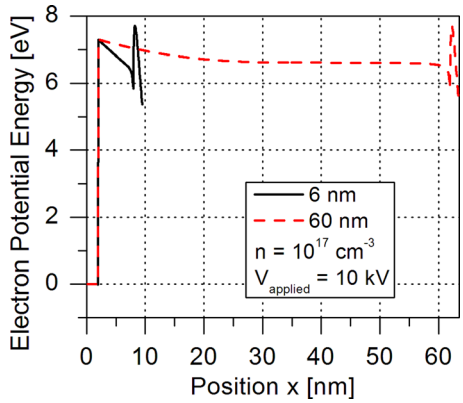

FIG. 9. Simulated electron potential energy as a function of position for a thin and a thick LaB_6 film at high applied field and low carrier density. The internal barrier is much thinner in the thin LaB_6 film case, resulting in increased tunneling and greater total field emission.

electrons can tunnel through the energy barrier at the internal interface, so emission is enhanced with respect to the metal cathode case due to the lower effective work function. For thick films, however, even though diffusion lowers the effective work function, the barrier at the internal interface does not become narrow enough to allow significant tunneling, as shown in Fig. 9, so emission is suppressed.

The simulated electron potentials for low carrier density coatings show that very thin (thick) films should enhance (suppress) field emission with respect to a bare metal cathode, in agreement with experimental findings. Experimental and simulation data indicate that the upper limit for the charge carrier density in our sputtered LaB_6 films is 10^{18} cm^{-3}.

Our study differs from the related work of Korotkov and Likharev[36] and Binh and Adessi.[37] Korotkov and Likharev[36] predicted enhanced emission through very thin cathode coatings due to resonant transmission. However, their thickest layers that yield current enhancement (~3 nm) are several times thinner than the layers in our study; as a result, resonant transmission alone is unlikely to be the sole reason for current enhancement in our work. The work of Binh and Adessi[37] is methodologically similar to ours: we solve Poisson's equation under the quasi-equilibrium condition and explain the findings in terms of band bending in the thin coating layer. Two important differences between the works are the material used for the thin emitter layer (semimetallic LaB_6 in this study versus wide-gap semiconductor) and the coating thicknesses considered (6–300 nm here versus 2–10 nm). Moreover, we also observe degradation of emission current for thicker layers of LaB_6, which is a very good emitter material otherwise.

VI. CONCLUSIONS

Field emission from sputtered LaB_6 coatings exhibits a strong dependence on the coating thickness. We find experimentally that emission from knife-edge cathodes is enhanced by sputter-coating them with a thin layer of LaB_6 (<10 nm) and that emission from knife-edge cathodes is suppressed by sputter-coating them with a thick LaB_6 layer. Numerical

Downloaded 19 Apr 2012 to 128.104.180.67. Redistribution subject to AIP license or copyright; see http://jap.aip.org/about/rights_and_permissions

calculations of the electrostatic potential in the system show that, in thinly coated samples, electrons tunnel efficiently through both the internal and external barrier, resulting in current enhancement with respect to the uncoated case. However, the thick internal barrier in thickly coated samples suppresses current below the value for uncoated samples despite the lowered external barrier. This internal barrier width variation occurs because the as-deposited LaB_6 films are actually poor conductors and create a Schottky-type junction at the internal interface rather than an Ohmic contact with the metal. We conclude that the dependence of emission on the coating thickness stems from a relatively low ($<10^{18}$ cm^{-3}) free carrier density in the sputtered polycrystalline LaB_6.

ACKNOWLEDGMENTS

This work was supported in part by U.S. DoD MURI04 AFOSR Grant No. FA950–04–0369 on the Nanophysics of High Current Density Cathodes and Window Breakdown, AFOSR Grant No. FA9550–09–1–0086 on Basic Studies of Distributed Discharge Limiters for Counter-HPM, AFOSR Award No. FA9550–08–1–0052, and by the NSF, Award Nos. ECCS-0547415 and DMR-0520527 (the University of Wisconsin MRSEC). The authors would like to thank J. Scharer and Ryan Jacobs for helpful discussions and Rebecca Bauer, Bill Cotter, and Don Savage for assistance with sample preparation and materials characterization measurements.

[1]R. J. Barker, J. H. Booske, N. C. Luhmann, and G. S. Nusinovich, *Modern Microwave and Millimeter-Wave Power Electronics* (IEEE Press, New York, 2005).
[2]R. H. Fowler and L. Nordheim, Proc. R. Soc. London, Ser. **A119**, 173–181 (1928).
[3]K. L. Jensen, J. Vac. Sci. Technol. B **21**,1528 (2003).
[4]J. M. Lafferty, J. Appl. Phys. **22**, 299–309 (1951).
[5]X. Wang, Y. Jiang, Z. Lin, K. Qi, and B. Wang, J. Phys. D: Appl. Phys. **42**, 1–4 (2009).
[6]D. M. Goebel, Y. Hirooka, and T. A. Sketchley, Rev. Sci. Instrum. **56**, 1717 (2009).
[7]Y. Kato, Y. Ono, Y. Akita, M. Hosaka, N. Shiraishi, N. Tsuchimine, S. Kobayashi, and M. Yoshimoto, MRS Symp. Proc. **1148**, 12–02 (2008).
[8]M. E. Herniter and W. D. Getty, IEEE Trans. Plasma Sci. **18**, 992–1001 (2002).
[9]D. J. Late, M. A. More, D. S. Joag, P. Misra, B. N. Singh, and L. M. Kukreja, in Vacuum Nanoelectronics Conference, 2006 and the 2006 50th International Field Emission Symposium., IVNC/IFES 2006. Technical Digest. 19th International (2007), pp. 111–112.
[10]C. Mitterer, J. Solid State Chem. **133**, 279–291 (1997).
[11]S. J. Mroczkowski, J. Vac. Sci. Technol. A **9**, 586–590 (1991).
[12]W. Waldhauser, C. Mitterer, J. Laimer, and H. Störi, Surf. Coat. Technol. **98**, 1315 (1998).
[13]W. Waldhauser, C. Mitterer, J. Laimer, and H. Störi, Surf. Coat. Technol. **74**, 890 (1995).
[14]K. R. Peschmann, J. T. Calow, and K. G. Knauff, J. Appl. Phys. **44**, 2252–2256 (1973).
[15]S. Winsztal, H. Majewska-Minor, M. Wisniewska, and T. Niemyski, Mater. Res. Bull. **8**, 1329 (1973).
[16]W. Wei, K. Jiang, Y. Wei, P. Liu, K. Liu, L. Zhang, Q. Li, and S. Fan, Appl. Phys. Lett. **89**, 203112 (2006).
[17]D. J. Late, S. Karmakar, M. A. More, S. V. Bhoraskar, and D. S. Joag, J. Nanopart. Res. **12**, 2393–2403 (2009).
[18]Chemical Rubber Company, *CRC Handbook of Chemistry and Physics*, Electronic ed. (CRC Press, Boca Raton, FL).
[19]K. H. J. Buschow, R. W. Cahn, M. C. Flemings, B. Ilschner, E. J. Kramer, and S. Mahajan, *Encyclopedia of Materials - Science and Technology, Volumes 1–11* (Elsevier).
[20]H. Yamauchi, K. Takagi, I. Yuito, and U. Kawabe, Appl. Phys. Lett. **29**, 638 (1976).
[21]M. D. Williams, L. T. Jackson, D. O. Kippenhan, K. N. Leung, M. K. West, and C. K. Crawford, Appl. Phys. Lett. **50**, 1844 (1987).
[22]T. Tanaka, T. Akahane, E. Bannai, S. Kawai, N. Tsuda, and Y. Ishizawa, J. Phys. C **9**, 1235 (1976).
[23]J. H. Luscombe and A. M. Bouchard, Phys. Rev. B **46**, 10262–10268 (1992).
[24]L. D. Landau and E. M. Lifshits, *Quantum Mechanics, Non-Relativistic Theory*, 3rd ed. (Beijing World Publishing, Beijing, 1999).
[25]W. R. Frensley, Rev. Mod. Phys. **62**, 745–790 (1990).
[26]E. L. Murphy and R. H. Good, Phys. Rev. **102**, 1464 (1956).
[27]M. Lundstrom, *Fundamentals of Carrier Transport* (Cambridge University Press, Cambridge, 2000).
[28]P. F. Walch, D. E. Ellis, and F. M. Mueller, Phys. Rev. B **15**, 1859–1866 (1977).
[29]A. Arko, G. Crabtree, D. Karim, F. Mueller, L. Windmiller, J. Ketterson, and Z. Fisk, Phys. Rev. B **13**, 5240 (1976).
[30]E. H. Hygh and R. M. Welch, Phys. Rev. B **1**, 2424–2430 (1970).
[31]R. M. Welch and E. H. Hygh, Phys. Rev. B **4**, 4261 (1971).
[32]R. M. Welch and E. H. Hygh, Phys. Rev. B **9**, 1993–1996 (1974).
[33]O. Jepsen, Phys. Rev. B **12**, 2988–2997 (1975).
[34]P. J. Feibelman, J. Appelbaum, and D. Hamann, Phys. Rev. B **20**, 1433–1443 (1979).
[35]Z. W. Lu, D. Singh, and H. Krakauer, Phys. Rev. B **36**, 7335 (1987).
[36]A. N. Korotkov and K. K. Likharev, Appl. Phys. Lett. **75**, 2491 (1999).
[37]V. T. Binh and C. Adessi, Phys. Rev. Lett. **85**, 864–867 (2000).

Downloaded 19 Apr 2012 to 128.104.180.67. Redistribution subject to AIP license or copyright; see http://jap.aip.org/about/rights_and_permissions